Optimal control of bidirectional active clamp forward converter with synchronous rectifier based cell-to-external-storage active balancing system

Kai Shi*, Truong Bui, James Marco

Warwick Manufacturing Group, University of Warwick, Coventry, UK, CV4 7AL

Abstract

Active cell balancing is a more energy-efficient way of balancing cells in series comparing to passive balancing. To further improve the performance of an active balancing system, an optimal control approach can be applied to optimise the system performance indexes. This paper proposes an optimal controller for the bidirectional active clamp forward converter with synchronous rectifier (ACFC-SR) based cell-to-external-storage active balancing system to concurrently optimise the balancing speed and the energy efficiency. The formulated optimization problem does not require a complicated nonlinear converter efficiency model compared to other optimal controllers that involve efficiency model to reduce energy loss. The flexibility in changing the balancing priority of the balancing time and the converter efficiency is achieved via different weights on the objective function. The effectiveness of the proposed controller is validated experimentally with real cells and the power electronics board.

Keywords: active cell balancing, optimal control, model predictive control, dc-dc converter, converter efficiency

*Corresponding author

Email address: kai.shi@warwick.ac.uk (Kai Shi)

1. Introduction

Lithium-ion batteries have been widely used as a power source because of their high energy density compared to other commonly used batteries like lead-acid, Ni-Cd, and Ni-MH batteries. In high voltage applications, e.g. electric vehicles, several battery cells are connected in series to meet the high voltage output requirement [1, 2, 3, 4, 5]. A battery module that consists of cells in series can become unbalanced over time due to the different ageing rate of the cells [6, 7, 8]. The ageing process would change the self-discharge current, increase internal resistance, and reduce the cell capacity of a cell. Different ageing speed of the cells in a battery module increases the cell-to-cell variations and results in large imbalances among cells. Generally, those imbalances are considered inevitable and result in the reduction of the effective energy capacity of the battery module [9]. The effective energy capacity of a module without a balancing system is limited by the minimum remaining charge in cells that can be discharged and the minimum cell capacity that can be charged as cells in series can neither be fully charged nor discharged [10]. A cell balancing system, which is either passive or active, is capable of equalising the state-of-charge (SOC) of cells such that more charge stored in cells are available for discharge and the effective module capacity can be increased. The passive balancing system removes charges until all cell SOCs are equalised, it is usually applied during the charging process to fully charge every cell [11]. The excess energy in a cell is dissipated through an external resistor as heat, which is a waste of energy and the balancing speed is slow as a result of reducing balancing current to maintain efficiency. Another drawback of the passive balancing system is that it does not help to increase the effective capacity of a module during the process of discharging. Active balancing is a more energy-efficient way of balancing the cells comparing to the passive balancing methods as it redistributes energy among cells instead of dissipating it. The active balancing system works for both charging and discharging processes. In the charging process, the active balancing system ensures each cell to be fully charged with less energy being wasted than using the passive balancing system. When a module is under a discharging operation, it can increase the effective capacity of a module with unbalanced cells.

Research on active balancing system focuses on the design of the balancing hardware and the control strategy. Several indexes have been considered to evaluate the performance of an active balancing system, such as the hardware cost, balancing speed, energy efficiency, and effective capacity etc. For the balancing hardware, the realisation of active balancing relies on the application of power electronics. Several active balancing topologies have been proposed to achieve energy redistribution among cells, the review of different active balancing topologies is available in [12]. The design of the control strategy of an active balancing system includes a low-level control of the power electronics to regulate the balancing current, which depends on the balancing circuit topology, and a high-level control of battery cells to decide the balancing current of each cell subject to environmental conditions and external factors, such as temperature, electrical load conditions etc. With the same balancing hardware, different control strategies would affect the balancing speed and energy efficiency. The rule-based control is commonly used in the active balancing system because it has a simple structure and low computational cost [13, 14, 15, 16]. However, those simple rule-based controllers do not optimise the performance indexes such as the balancing time, the energy loss, and the effective energy capacity etc, hence the performance of the active balancing system is not maximised. The approach of optimal control allows the control system to optimise the performance indexes via minimising a defined objective function. In [17] an optimal control approach is proposed to maximise the effective capacity whereas the balancing time is chosen as the objective function to be minimised in [18]. Both [17] and [18] do not consider the energy efficiency of the balancing circuit. In [19] the efficiency model of the power electronics converter is included in the objective function, but only two-cell balancing is studied. The efficiency of a power electronics converter is a nonlinear function of the terminal voltage and the current [20, 21, 22]. Involving the efficiency model in the optimisation problem formulation may increase the computational cost and make the problem difficult to be solved, this would challenge the active balancing system when there are plenty of cells that need to be balanced. Moreover, the objective that maximises the balancing speed may contradict the objective that maximises the energy efficiency, as the fast balancing speed normally requires a large balancing current that is far away from the optimal point, at which the efficiency is maximum. The trade-off between the balancing speed and the energy efficiency needs to be considered for different operating conditions.

The bidirectional ACFC-SR based cell-to-external-storage active balancing system is an alternative dc-dc converter based active balancing topology but it has been investigated by few researchers. The system of bidirectional ACFC-SR based cell-to-external active balancing system is shown in Fig.1. Different from the multiple dc-dc converters based active balancing system in [18], which uses one dc-dc converter for one cell individually, the cells connected to bidirectional ACFC-SR active balancing system share one dc-dc converter via a switching matrix. This topology uses fewer converters that simplify the power electronics circuit and reduce the costs. Two similar topologies can be found in [23] and [24]. In [23], the cells share the dc-dc converter via switching matrix and two of the cells in series can be connected to exchange energy at one time. The converter modelling and formulation of the efficiency is discussed but the designed rule-based controller does not consider the energy efficiency. In [24] the energy movement to balance the battery is achieved via a bidirectional dc-dc converter with an auxiliary battery, but the energy efficiency is not considered in the controller design either.

This paper proposes an optimal control based active cell balancing strategy that considers both the balancing speed and the converter efficiency in one objective function. The nonlinear efficiency model is not required in the optimisation problem such that the computational costs are low while the goal of increasing the efficiency still can be achieved by tracking the optimal balancing current. The weights are added to the objective function so the controller provides the flexibility of changing the priorities of each control objectives. The cell-to-external-storage topology of the active balancing system is used as a case study to evaluate the proposed optimal controller.

The rest of this paper is structured as follows. Section 2 introduces the cell-to-external topology of the active balancing system and the modelling, Section 3 presents the proposed optimal controller, Section 4 discusses the experiment results, and Section 5 draws the conclusion.

2. Model of the Bidirectional ACFC-SR based Cell-to-External Active Balancing System

The active balancing with the system shown in Fig.1 is performed via exchanging energy between the battery cells and an external power source. All cells connected to the system share one bidirectional dc-dc converter, which uses bidirectional ACFC-SR in this paper. A switching matrix is controlled to make sure only one cell is connected to the dc-dc converter at one time for charging/discharging. The peak current mode control is applied to regulate the balancing current while this paper focuses on the active balancing strategy that generated the balancing current commands. The operation principle, dynamic modelling, and the power loss analysis of the bidirectional ACFC-SR based active balancing system can be found in our previous research work [25, 26] so it will not be introduced in detail here. In the rest of this section, the model of the active balancing system is introduced.

The SOC of a cell denotes the current charge level as a fraction of the rated capacity of charge. The value of the SOC is defined between 0 and 1, $SOC = 1$ represents that the cell is fully charged and $SOC = 0$ suggests that the cell is fully discharged. The SOC can be modelled by coulomb counting, which integrates the cell current over time and is given by

$$SOC\left(t\right) = SOC\left(0\right) + \frac{1}{3600Q_0}\int_0^t i\left(\tau\right)d\tau \tag{1}$$

where Q_0 is the value of charge when $SOC = 1$ in $Ampere - hour(Ah)$.

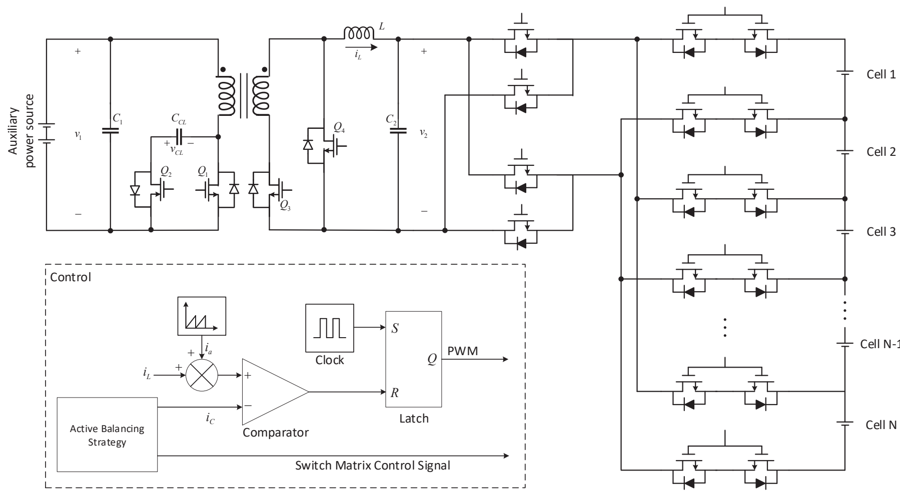

Figure 1: Bidirectional ACFC-SR based cell-to-external active balancing system

Considering n cells connected in series, the state equation of the cell SOCs in vector form can be obtained based on (1) as

$$\dot{x} = \frac{1}{3600} Q^{-1} \left(S i_b + I \right) \tag{2}$$

The definitions of the variables and parameters are given as follows. $x = [x_1, x_2, ..., x_n]^T$ denotes the vector of cell SOCs. $i_b = [i_{b1}, i_{b1}, ..., i_{bn}]^T$ denotes the vector of the balancing current that is defined as the input of the active balancing control system. Q is a $n \times n$ diagonal matrix defining the charge capacities:

$$Q = \begin{bmatrix} Q_1 & 0 & \cdots & 0 \\ 0 & Q_2 & \cdots & 0 \\ \vdots & \vdots & \ddots & \vdots \\ 0 & 0 & \cdots & Q_n \end{bmatrix} \tag{3}$$

in which $Q_1 ... Q_n$ denote the charge capacities of cell 1 to cell n. S is a $n \times n$ diagonal matrix that describes the behaviour of the switching matrix in the cell-to-external-storage active balancing system:

$$S = \begin{bmatrix} s_1 & 0 & \cdots & 0 \\ 0 & s_2 & \cdots & 0 \\ \vdots & \vdots & \ddots & \vdots \\ 0 & 0 & \cdots & s_n \end{bmatrix} \tag{4}$$

in which $s_1, ..., s_n \in \{0, 1\}$ denote the "ON-OFF" status of of the switches between cell and converter. If $s_i = 1$, the ith cell is connected to the dc-dc covnerter. Those swithcing signals are constrainted by $\sum\limits_{i=1}^{N} s_i = 1$ for the cell-to-external-storage topology studied in this paper as one dc-dc converter is shared by all of the cells; $I = [I_1, I_2, ..., I_3]^T$ denote the cell currents due to charging/discharging of the battery module. As those n cells are connected in series, it is assumed that $I_1 = I_2 = \cdots = I_n$. u denotes the balancing current.

To implement the dynamical system (2) in discrete time, the forward Euler method can be applied to convert the dynamic equation (2) in continuous-time to a discrete-time one:

$$x\left(k+1\right) = x\left(k\right) + \frac{T_s}{3600} Q^{-1} \left(S i_b\left(k\right) + I\right) \tag{5}$$

where T_s is the sample time, which is $1s$ in this study.

Similarly, the dynamic equation of the SOC external-storage battery in discrete-time can be written as

$$z\left(k+1\right) = z\left(k\right) + \frac{T_s}{3600} {Q_z}^{-1} i_z\left(k\right) \tag{6}$$

where z denotes the SOC of the external battery, Q_z denotes the charge capacity, i_z denotes the current of the external battery. With the efficiency model of the dc-dc converter,i_z can be estimated by

$$I_b = \sum_{l=1}^{n} S_l i_{bl} \tag{7}$$

$$i_z = \eta\left(I_b\right) \frac{V_1}{V_2} I_b \tag{8}$$

where V_1 is the voltage of the external battery and V_2 is the voltage of the cell that is connected to the dc-dc converter, and $\eta(u)$ is the efficiency function in terms of the balancing current. For the application of the bidirection ACFC-SR, the efficiency can be modelled by

$$\eta(u) = \begin{cases} \eta_1(u) & u > 0 \\ \eta_2(u) & u < 0 \\ 0 & u = 0 \end{cases} \tag{9}$$

where $\eta_1(u)$ stands for the efficiency function of the converter for charging operation ($u > 0$) and $\eta_2(u)$ is the efficiency function of the converter for discharging operation ($u < 0$). The detailed power loss analysis and efficiency model for the bidirectional ACFC-SR system can be found in [26]. When implementing the system with hardware, the current of the external source can also be obtained via sensor measurement.

3. Optimal Control Design

3.1. Formulation of the objective function

The main objective of an active balancing system is to remove the cell imbalances and maintain a balanced condition among cells. In this study, the SOC based active balancing is considered and the SOC can be estimated using the Columb counting method, which is not discussed in this paper. For SOC based balancing, it is common to refer to the status of imbalance to the average SOC. The cells are considered to be balanced if the SOC of each cell equals to the average SOC, namely $x_i = \frac{1}{n}\sum_{i=1}^{n} x_i, i = 1, ..., n$. The condition of balanced SOC can be rewritten in matrix form as

$$Lx = 0 \tag{10}$$

where

$$L = \begin{bmatrix} 1-\frac{1}{n} & -\frac{1}{n} & \cdots & -\frac{1}{n} \\ -\frac{1}{n} & 1-\frac{1}{n} & \cdots & -\frac{1}{n} \\ \vdots & \vdots & \ddots & \vdots \\ -\frac{1}{n} & -\frac{1}{n} & \cdots & 1-\frac{1}{n} \end{bmatrix} \tag{11}$$

The objective function that represents the status of imbalance is then defined as

$$J_1 = (Lx)^T (Lx) \tag{12}$$

The second objective is to let the converter keep working at maximum efficiency. It can be achieved by regulating the magnitude of the balancing current to the optimal balancing current reference that results in maximum efficiency. The complete objective function for maximising the converter efficiency can be defined as

$$J_2 = (|i_b| - I_{opt})^T (|i_b| - I_{opt}) \tag{13}$$

where I_{opt} denotes the optimal value of the balancing current that results in a maximum efficiency when it is applied.

Apart from the objectives J_1 and J_2, the cell-to-external-storage active balancing topology needs to maintain the charge level of the external battery, ideally, the SOC of the external battery at the time when balancing is finished equals to its initial condition. The related cost function can be defined as

$$J_3 = (z - z_0)^2 \tag{14}$$

where z_0 denotes the initial SOC of the external battery.

Combining (12), (13), and (14), the final objective function for can be written as

$$J = w_1 J_1 + w_2 J_2 + w_3 J_3 \tag{15}$$

where w_1, w_2, w_3 are weights of the objective functions that affect the priority of each objective.

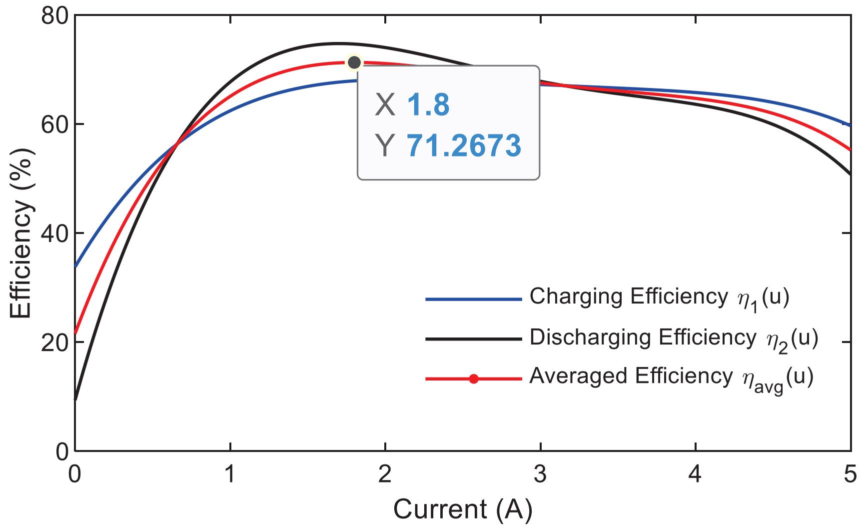

Figure 2: Efficiency curve for charging and discharging operations.

3.2. Determination of the Optimal Current I_{opt}

The optimal value of the balancing current can be determined based on the efficiency curve, which can either be obtained by mathematical modelling or experiment tests. In this paper, the efficiency curve of the TI EM1402 active balancing board obtained from experiment tests is used as the case study. In this paper, the power loss on the active balancing system is considered, including the loss on power electronics components, transformers, passive components, and wirings. The efficiency curve is obtained via measurement of the system input/output voltages and currents, which avoids the inaccuracy using model based estimations due to the parameter uncertainty. The efficiency curves with respect to the currents for the charging and discharging operations are shown in Fig.2. To reduce the complexity of the optimisation problem, the average efficiency curve is introduced by $\eta_{avg} = (\eta_1 + \eta_2)/2$. Then the maximum efficiency of the averaged curve and the optimal balancing current value can be obtained. In this paper, the optimal balancing current is chosen to be $I_{opt} = 1.8$ that results in 71.27% averaged converter efficiency.

3.3. Model Predictive Control (MPC)

The model predictive control is applied to perform the online optimisation at each time step to minimise the cost function. To implement the MPC, M is defined as the prediction horizon and the control horizon is set to be equal to the prediction horizon in this paper. The predictive states at kth time instant can be expressd as $x\left(k+i\left|k\right.\right), i=1,...,M$ and $z\left(k+i\left|k\right.\right), i=1,...,M$, and the control inputs at kth time instant is given by $u\left(k+i-1\left|k\right.\right) i=1,...,M$. The cost function at kth time instant can then be writtern as

$$\begin{aligned} J\left(k+i\left|k\right.\right) = w_1 J_1\left(k+i\left|k\right.\right) + w_2 J_2\left(k+i\left|k\right.\right) \\ + w_3 J_3\left(k+i-1\left|k\right.\right) \end{aligned} \tag{16}$$

Then, the optimisation problem to be solved at kth time instant with constraints can be written as

$$\begin{aligned} J^* = \min \sum_{i=1}^{M} \left[w_1 J_1\left(k+i\left|k\right.\right) + w_2 J_2\left(k+i\left|k\right.\right) \right. \\ \left. + w_3 J_3\left(k+i-1\left|k\right.\right) \right] \end{aligned} \tag{17}$$

Subject to

$$\begin{aligned} x\left(k+i\left|k\right.\right) = x\left(k+i-1\left|k\right.\right) \\ + \tfrac{T_s}{3600} Q^{-1}\left(S i_b\left(k+i-1\left|k\right.\right) + I\right) \end{aligned} \tag{18}$$

$$\begin{aligned} z\left(k+i\left|k\right.\right) = z\left(k+i-1\left|k\right.\right) \\ + \tfrac{T_s}{3600} {Q_z}^{-1} i_z\left(k+i-1\left|k\right.\right) \end{aligned} \tag{19}$$

$$I\_CELL\_MIN \leq i_b\left(k+i-1\left|k\right.\right) + I \leq I\_CELL\_MAX \tag{20}$$

$$I_b\left(k+i-1\left|k\right.\right) = \sum_{l=1}^{n} S_l i_{bl}\left(k+i-1\left|k\right.\right) \tag{21}$$

$$i_z\left(k+i-1\left|k\right.\right) = \eta\left(I_b\left(k+i-1\left|k\right.\right)\right) \frac{V_1}{V_2} I_b\left(k+i-1\left|k\right.\right) \tag{22}$$

$$0 \leq x\left(k+i\left|k\right.\right) \leq 1 \tag{23}$$

$$0 \leq z\left(k+i\left|k\right.\right) \leq 1 \tag{24}$$

In (20), I_CELL_MIN and I_CELL_MAX are the lower and higher limits of the cell current set to guarantee the safe operations, the values of the limits can be found from the datasheet of the active balancing board provided by the manufacturer. It should be noted that the values switching matrix S are determined by a fixed switching logic in order to further reduce the complexity of the optimisation problem. In this paper, each switch $s_i, i \in 1...n$ is ON for 1 second in a period of n seconds and the switches turn on in order from s_1 to s_n. Since only one converter is shared by all of the cells in series, only one switch is on at one time.

4. Experimental Validation

The effectiveness of the proposed control strategy is validated by experiment with the set-up shown in Fig.3. TI EM1402 power electronics boards with the balancing topology given in Fig.1 are used as the active balancing circuit and the cell monitoring unit. A dSPACE SCALEXIO is used to implement the control algorithm in real-time and output the control command signals (balancing current values) to a TI TMS570 launchpad via CAN bus. Then the TI launchpad controls the switching matrix IC and the dc-dc converter on the active balancing board to balance the cells. There are 14 lithium-ion cells (LG M50) connected in series and initialised to randomly generated SOC values before starting the tests. A programmable power supply is employed to charge/discharge the cells in series with a pre-set current profile of the Artemis drive cycle (shown in 4)until one of the cells reaches the cut-off condition. The actual efficiency of the active balancing system and the energy loss are obtained via measuring the voltages and currents at the input/output terminals of the active balancing system.

Comparison study is conducted experimentally to evaluate the performance of the proposed controller. The details of those controllers are listed as follows.

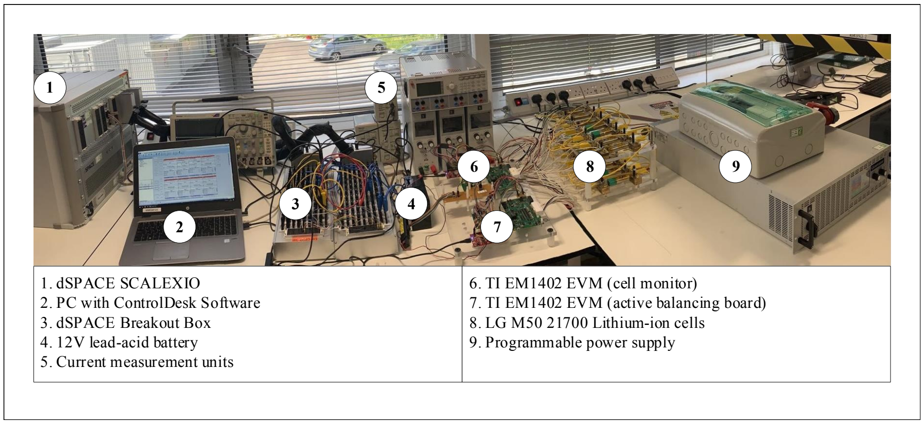

Figure 3: Experiment setup

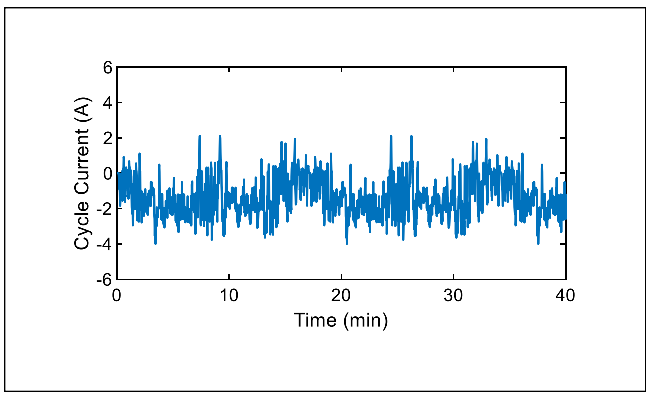

Figure 4: Current profile of the Artemis drive cycle

- RBC-1A: a rule-based controller that converges the SOC of the cells to the average value with a fixed 1A balancing current.
- RBC-4A: a rule-based controller that converges the SOC of the cells to the average value with a fixed 4A balancing current.
- OPC: An optimal control without consideration of the efficiency, this is equivalent to minimising the objective function (15) with $w_2 = 0$.
- OPCE: The proposed controller with consideration of the energy efficiency using the objective function (15).

The lihium-ion cells have been characteristics and the charge capacity of the cells are 4.8654 Ah, 4.8812 Ah, 4.8452Ah, 4.8358Ah, 4.8242Ah, 4.8785Ah, 4.8747Ah, 4.8735Ah, 4.8563Ah, 4.8670Ah, 4.8571Ah, 4.8513Ah, 4.8714Ah, and 4.9076Ah. The random values generated for the initial SOC of the cells are: 0.7700, 0.8300, 0.7000, 0.8500, 0.7500, 0.7800, 0.8200, 0.8700, 0.7000 0.8600, 0.7300, 0.8600, 0.7800, and 0.7100. With information of the cell capacities and initial SOCs, coulomb counting is applied to estimate the real-time cell SOCs during testing. The weightss of the optimal controllers are chosen as $w_1 = 4000, w_2 = 0.005, w_3 = 1000$ for the proposed controller (OPCE) and $w_1 = 4000, w_2 = 0, w_3 = 1000$ for the OPC. In this paper, the weights are selected manually: increasing w_1 will pay more effort to equalise the cell SOCs hence to reduce the time to balance while increasing w_2 will result in a balancing current closer to the optimal current thus has a better efficiency during operation and smaller power loss. The sample rate of the controller is chosen as $14s$ as each cell is connected to the active balancing board for 1s to be charged/discharged in one control cycle so one cycle (all cells to be connected to the active balancing board once) lasts $14s$. To prevent cells from being over-discharged, the cut-off voltage is set as $2.5V$ and the cut-off SOC is set as 0.002. To avoid over-balancing of the system, the all controllers will stop balancing the cells when $J_1 < 1e-4$ and the active balancing can resume if J_1 exceed the threshold again.

The experiment results of the active balancing control with four controllers are presented in Fig.5 and the comparison of the active balancing performance is shown in Fig.6. The quantitative comparison of the performance is given in Table1. Fig.5(a) shows that the RBC-1A fails to equalise the cell SOCs when the cells stop discharging as significant unbalanced cell voltages and SOCs can be observed, whereas the other three controllers manage to converge the SOCs and decrease J_1 below the threshold. The testing results indicate that the OPC has the shortest time to balance and the OPCE takes the longest time to equalise the SOCs. The balancing speed closely relates to the balancing current as a large current can charge/discharge cells to the desired SOC level faster than small currents. The RBC-1A and RBC-4A are with fixed pre-set balancing

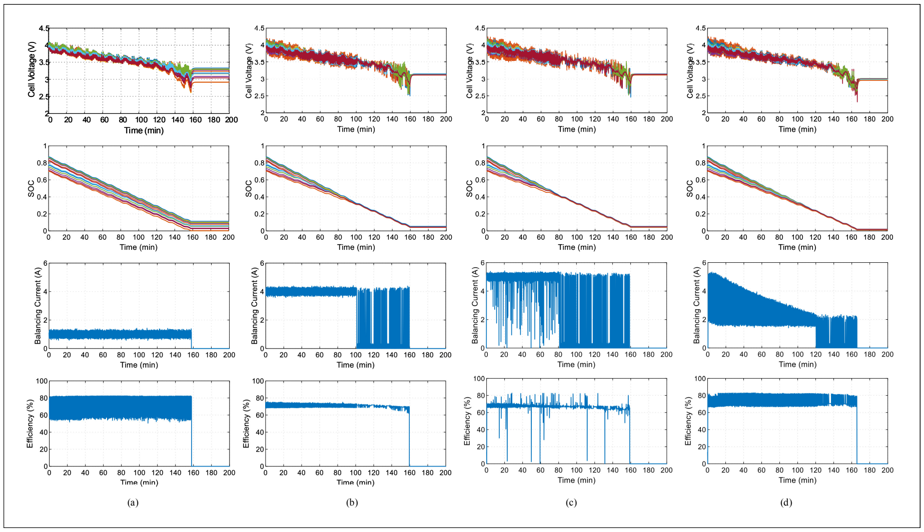

Figure 5: Experiment results of the active balancing tests with different cotnrollers: (a) RBC-1A, (b) RBC-4A, (c) OPC, (d) OPCE.

current while the balancing currents of the OPC and OPCE are determined by the controller. The OPC pays a lot of effort on SOC equalisation such that the resulted balancing current is around the upper limit of the active balancing board ($5A$) and triggers the build-in over-current protection that causes some drops of the balancing currents during the process of active balancing. It can also be observed in Fig.6(c) that the OPC provides a faster reduction speed in J_1 than others. The OPCE applies a large balancing current at the beginning of the balancing when the SOC difference among cells is large and gradually reduces it to be close to the optimal current when the SOC difference becomes smaller. As the capacity of each cell varies, the cells in series with equalised SOCs will become unbalance again after being equalised, thus the controller starts to balance cells again when J_1 is detected larger than the threshold value ($1e - 4$).

With respect to the energy performance of the active balancing controllers, Fig.6 and Table1 suggest that the proposed OPCE is the most energy-efficient with $7.0Wh$ energy loss and extracts $186Wh$ of energy to the load. The total extracted energies of RBC-1A, RBC-4A, and OPC are close even though the RBC-1A does not equalise the cell SOCs. The reason is that RBC-4A and OPC apply high balancing currents to the cells and cause large energy losses, which are $9.1Wh$ and $10.9Wh$, respectively. The energy loss with RBC-1A is less than half of the energy loss caused by either RBC-4A or OPC. Although the RBC-4A and OPC provide a good performance of fast balancing, the large energy loss will reduce the available energy for the load. To maximise the total available energy of the cells is one of the most important targets of active balancing, the fast active balancing strategies will be less effective if there is no increase in total energy outputs due to the large energy loss. By optimising the balancing current, the OPCE is able to operate close to high-efficiency points of the converter (average 0.74 in the tests) as well as converge the SOCs to fully discharge all cells at the same time, and it extracted $186Wh$ from the cells to the load which is the most among these four controllers.

To sum up, there is a trade-off between the balancing current and the power loss as the high balancing current would cause high power loss. On the contrary, a small balancing current may have good energy efficiency but can be too slow to balance the cells before the end of discharge such that the remaining energy stored in cells can not be extracted. The RBC-4A and OPC are with high balancing current hence the fast equalisation speed but cause large energy loss at the same time. The RBC-1A has low energy loss however it fails to fully discharge most of the cells so the system cannot use up all energy stored in cells. The comparison shows that the performance of the proposed OPCE is optimal as it varies the balancing current while minimising the cost function with consideration of both equalisation speed and energy efficiency. Furthermore, the proposed OPCE does not require the complicated nonlinear converter efficiency model so the computational cost is smaller comparing to other efficiency model based optimisations. The optimum current value can be obtained from experiment tests to avoid the influence of the parameter uncertainties on efficiency-model based methods.

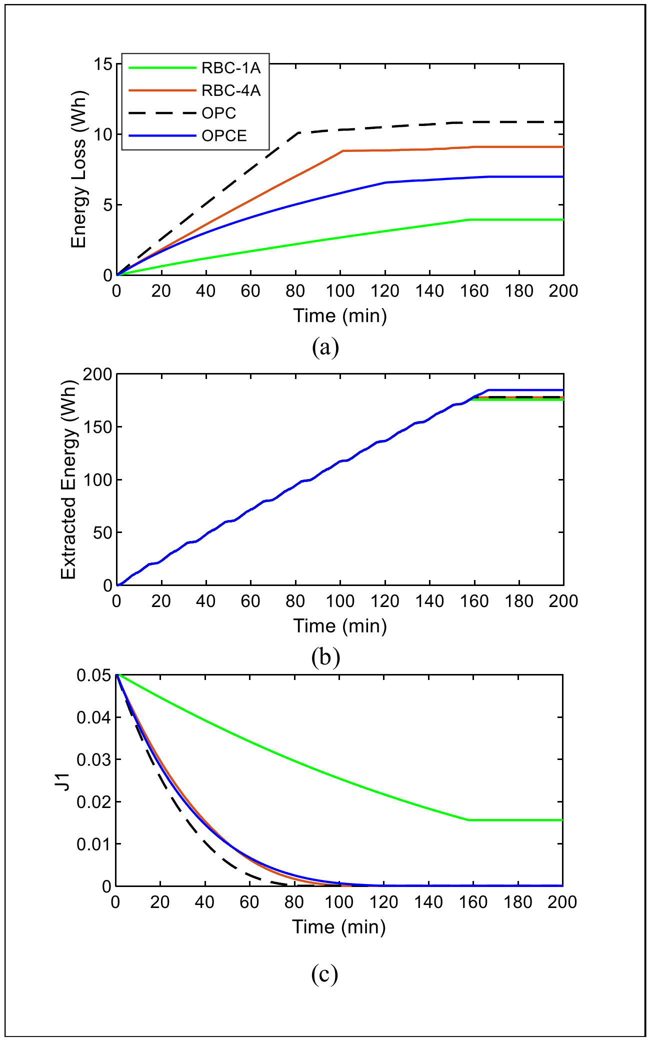

Figure 6: Active balancing performance comparison

5. Conclusion

In this paper, the optimal control strategy that optimises the trade-off between the equalisation speed and the converter efficiency has been proposed for the cell-to-external-storage based active cell balancing system. An objective function has been defined to minimise the imbalance of the cell SOCs and track the optimal balancing current value. The optimal balancing current value

Table 1: Comparison of the active balancing performance.

	Time to balance (min) (when J1<1e-4 for the first time)	Energy Loss (Wh)	Extracted Energy (Wh)	Final SOC Standard Deviation	Average Effeciency
RBC-1A	-	3.9	175	0.0347	0.706
RBC-4A	100.9	9.1	177	0.0027	0.707
OPC	80.9	10.9	178	0.0025	0.667
OPCE	120.3	7.0	186	0.003	0.741

can be obtained via the converter efficiency curves from experimental tests so there is no need to integrate a complicated nonlinear efficiency model into the optimisation problem formation. The trade-off between the balancing time and energy efficiency can be balanced by selecting proper weights for the objective function to slow down the balancing speed and operates the converter with high efficiency such that more energy can be extracted from the cells to the load.

The future research will be conducted to furtherly investigate the effects on different weights in the objective function and the optimal weight tuning methods. The proposed strategy will also be applied to other dc-dc converter based active balancing topologies to evaluate the energy performance of the proposed controller on different systems. Since the proposed controller relies on the accuracy on the SOC and capacity estimation, the impact of the inaccuracy in SOC estimator and capacity data on the controller performance is necessary to be studied.

Acknowledgements

This work was undertaken in collaboration with the High Value Manufacturing Catapult, part-funded by Innovate UK.

References

[1] N. H. Kutkut, D. M. Divan, D. W. Novotny, Charge equalization for series connected battery strings, IEEE Transactions on Industry Applications 31 (3) (1995) 562–568.

[2] N. Nguyen, S. K. Oruganti, K. Na, F. Bien, An adaptive backward control battery equalization system for serially connected lithium-ion battery packs, IEEE Transactions on Vehicular Technology 63 (8) (2014) 3651–3660.

[3] M. Einhorn, W. Guertlschmid, T. Blochberger, R. Kumpusch, R. Permann, F. V. Conte, C. Kral, J. Fleig, A current equalization method for serially connected battery cells using a single power converter for each cell, IEEE Transactions on Vehicular Technology 60 (9) (2011) 4227–4237.

[4] J. Gallardo-Lozano, E. Romero-Cadaval, M. I. Milanes-Montero, M. A. Guerrero-Martinez, Battery equalization active methods, Journal of Power Sources 246 (2014) 934 – 949. doi:https://doi.org/10.1016/j.jpowsour.2013.08.026.
URL http://www.sciencedirect.com/science/article/pii/S0378775313013669

[5] E. Chatzinikolaou, D. J. Rogers, Performance evaluation of duty cycle balancing in power electronics enhanced battery packs compared to conventional energy redistribution balancing, IEEE Transactions on Power Electronics 33 (11) (2018) 9142–9153.

[6] F. Altaf, B. Egardt, Comparative analysis of unipolar and bipolar control of modular battery for thermal and state-of-charge balancing, IEEE Transactions on Vehicular Technology 66 (4) (2017) 2927–2941.

[7] D. Andrea, Battery management systems for large lithium-ion battery packs, Artech House, 2010.

[8] M. Caspar, T. Eiler, S. Hohmann, Systematic comparison of active balancing: A model-based quantitative analysis, IEEE Transactions on Vehicular Technology 67 (2) (2018) 920–934.

[9] K. Lee, Y. Chung, C. Sung, B. Kang, Active cell balancing of li-ion batteries

using lc series resonant circuit, IEEE Transactions on Industrial Electronics 62 (9) (2015) 5491–5501. doi:10.1109/TIE.2015.2408573.

[10] Y. Zheng, L. Lu, X. Han, J. Li, M. Ouyang, Lifepo4 battery pack capacity estimation for electric vehicles based on charging cell voltage curve transformation, Journal of Power Sources 226 (2013) 33 – 41. doi:https://doi.org/10.1016/j.jpowsour.2012.10.057.

[11] N. H. Kutkut, D. M. Divan, Dynamic equalization techniques for series battery stacks, in: Proceedings of Intelec'96 - International Telecommunications Energy Conference, 1996, pp. 514–521. doi:10.1109/INTLEC.1996.573384.

[12] M. Daowd, N. Omar, P. Van Den Bossche, J. Van Mierlo, Passive and active battery balancing comparison based on matlab simulation, in: 2011 IEEE Vehicle Power and Propulsion Conference, 2011, pp. 1–7.

[13] X. Zheng, X. Liu, Y. He, G. Zeng, Active vehicle battery equalization scheme in the condition of constant-voltage/current charging and discharging, IEEE Transactions on Vehicular Technology 66 (5) (2017) 3714–3723.

[14] Chang-Hua Lin, Hsuan-Yi Chao, Chien-Ming Wang, Min-Hsuan Hung, Battery management system with dual-balancing mechanism for lifepo4 battery module, in: TENCON 2011 - 2011 IEEE Region 10 Conference, 2011, pp. 863–867.

[15] Feng Ran, Hao Xu, Yuan Ji, Jiaqi Qin, Wenhui Li, An active balancing circuit for lithium battery management system with optoelectronic switches, in: TENCON 2015 - 2015 IEEE Region 10 Conference, 2015, pp. 1–5.

[16] Y. Zheng, M. Ouyang, L. Lu, J. Li, X. Han, L. Xu, On-line equalization for lithium-ion battery packs based on charging cell voltages: Part 2. fuzzy logic equalization, Journal of Power Sources 247 (2014) 460 – 466. doi:https://doi.org/10.1016/j.jpowsour.2013.09.012.

URL http://www.sciencedirect.com/science/article/pii/S0378775313015036

[17] C. Danielson, F. Borrelli, D. Oliver, D. Anderson, M. Kuang, T. Phillips, Balancing of battery networks via constrained optimal control, in: 2012 American Control Conference (ACC), 2012, pp. 4293–4298.

[18] L. McCurlie, M. Preindl, A. Emadi, Fast model predictive control for redistributive lithium-ion battery balancing, IEEE Transactions on Industrial Electronics 64 (2) (2017) 1350–1357.

[19] J. Liu, Y. Chen, H. K. Fathy, Nonlinear model-predictive optimal control of an active cell-to-cell lithium-ion battery pack balancing circuit, IFAC-PapersOnLine 50 (1) (2017) 14483 – 14488, 20th IFAC World Congress. doi:https://doi.org/10.1016/j.ifacol.2017.08.2297.
URL http://www.sciencedirect.com/science/article/pii/S2405896317331087

[20] M. K. Kazimierczuk, Pulse-Width Modulated DC-DC Power Converters, 2nd Edition, Wiley, 2016.

[21] S. Xu, T. Zhang, Y. Yao, W. Sun, Power loss analysis of active clamp forward converter in continuous conduction mode and discontinuous conduction mode operating modes, IET Power Electronics 6 (6) (2013) 1142–1150. doi:10.1049/iet-pel.2013.0019.

[22] Q. M. Li, F. C. Lee, M. M. Jovanovic, Large-signal transient analysis of forward converter with active-clamp reset, IEEE Transactions on Power Electronics 17 (1) (2002) 15–24. doi:10.1109/63.988664.

[23] M. A. Hannan, M. M. Hoque, P. J. Ker, R. A. Begum, A. Mohamed, Charge equalization controller algorithm for series-connected lithium-ion battery storage systems: Modeling and applications, Energies 10 (9) (2017). doi:10.3390/en10091390.
URL https://www.mdpi.com/1996-1073/10/9/1390

[24] M. Daowd, M. Antoine, N. Omar, P. Lataire, P. Van Den Bossche, J. Van Mierlo, Battery management system—balancing modularization based on a single switched capacitor and bi-directional dc/dc converter with the auxiliary battery, Energies 7 (5) (2014) 2897–2937. doi:10.3390/en7052897.
URL https://www.mdpi.com/1996-1073/7/5/2897

[25] K. Shi, T. Q. Dinh, J. Marco, Dynamic modelling of the bidirectional active clamp forward converter with peak current mode control for active cell balancing, in: 2019 23rd International Conference on Mechatronics Technology (ICMT), 2019, pp. 1–7. doi:10.1109/ICMECT.2019.8932128.

[26] K. Shi, T. Q. Dinh, J. Marco, Power loss analysis of bidirectional acfc-sr based active cell balancing system, IFAC-PapersOnLine 53 (2) (2020) 12402–12409, 21th IFAC World Congress. doi:https://doi.org/10.1016/j.ifacol.2020.12.1285.
URL https://www.sciencedirect.com/science/article/pii/S2405896320316876